Acta Mechanica 39, 155—169 (1981)

ACTA MECHANICA

Application of the Green's Function Method to Thin Elastic Polygonal Plates*

By

H. Irschik and **F. Ziegler**, Wien, Austria

With 5 Figures

(*Received September 22, 1980*)

Summary — Zusammenfassung

Application of the Green's Function Method to Thin Elastic Polygonal Plates. Recently, the Green's function method has been applied successfully to problems of plane elasticity, using influence functions of some finite basic domain of simple geometrical shape, which contains the given one as a subdomain. The result of this formulation is a pair of integral equations, which have to be defined only along that part of the boundary not coinciding with the border of the basic domain.

A rather general formulation for the solution of bending of plates of arbitrary convex planform and loading is presented, where, for the sake of brevity, plates of polygonal shape are considered. The polygonal plate is embedded in a rectangular domain, thereby applying coincidence of boundaries as far as possible. Those boundary conditions in the actual problem, which are not already satisfied, lead to a pair of coupled integral equations for a density function vector with components to be interpreted as line loads and moments distributed in the basic domain along the actual boundary. Thus, the kernel is the corresponding Green's matrix. Hence, having solved the integral equations, deflections and stresses in the actual problem are explicitly known.

Solution of the integral equations is generally achieved by a numerical procedure.

The method is tested in example problems by considering a trapezoidal plate under various boundary conditions.

Anwendung der Methode der Greenschen Funktion auf dünne elastische Polygonplatten. Die Methode der Greenschen Funktion wurde in jüngster Zeit erfolgreich auf Probleme der ebenen Elastizitätstheorie angewendet. Dabei fanden Einflußfunktionen eines endlichen Grundbereiches einfacher geometrischer Form, der den gegebenen Bereich einschließt, Verwendung. Das Resultat dieser Formulierung ist ein Integralgleichungspaar, welches entlang dem Teil des Randes zu erstrecken ist, der nicht mit dem Rand des Grundbereiches bereits zusammenfällt.

Eine allgemein gehaltene Formulierung der Biegelösung von Platten mit konvexem Grundriß unter beliebiger Belastung wird angegeben, wobei allerdings der Kürze halber eine Beschränkung auf Polygonplatten erfolgt. Die Polygonplatte wird in einen Rechteckbereich eingebettet, wobei soviele Ränder wie möglich zusammenfallen sollen. Jene Randbedingungen des wirklichen Problems, welche dann noch nicht erfüllt sind, führen auf ein gekoppeltes Integralgleichungspaar für den Dichtefunktionsvektor, dessen Komponenten als im Grundbereich entlang der wirklichen Berandung verteilte Linienlasten und Linienmomente gedeutet werden. Damit wird der Kern zur korrespondierenden Greenschen

* Presented at the XVth Int. Congr. Theor. and Appl. Mechanics (IUTAM), Toronto 1980, by F. Z.

0001-5970/81/0039/0155/$03.00

Matrix. Weiters sind, nach Lösung der Integralgleichungen, Biegefläche und Spannungen des wirklichen Problems explizit bekannt. Die Lösung der Integralgleichungen erfolgt im allgemeinen numerisch.

Die Methode wird an Beispielen getestet, wobei eine Trapezplatte unter verschiedenen Randbedingungen untersucht wird.

Introduction

Recently, the Green's function method has been applied successfully to problems of plane elasticity, using influence functions of some finite basic domain of simple geometrical shape, which contains the given one as a subdomain. The result of this formulation is a pair of integral equations which have to be defined only along that part of the boundary not coinciding with the border of the basic domain. A review of this formulation and its advantages over standard boundary-integral equations methods and the Finite Element Method is given by Yu. A. Melnikov [1].

The method applied to plate bending problems seems to be extremely useful and is the subject of the paper. A rather general formulation for the solution of bending of homogeneous and isotropic Kirchhoff-plates of arbitrary convex planform and loading is presented, where, for the sake of brevity, plates of polygonal shape are considered. The polygonal plate is embedded in a rectangular domain, thereby applying coincidence of boundaries as far as possible.

The problem of the basic (rectangular) domain is well treated in the literature with respect to Green's function and arbitrary loadings. Deflections and stresses are presented by superposition of the solution in the basic domain and some homogeneous solutions.

The boundary conditions in the actual problem, which are not already satisfied, lead to a pair of coupled integral equations for a density function vector with components to be interpreted as line loads and moments distributed in the basic domain along the actual boundary. Thus, the kernel is the corresponding Green's matrix. The homogeneous solution in the basic domain corresponds to those line loadings. Hence, having solved the integral equations, deflections and stresses in the actual problem are explicitly known.

Solution of the integral equations is generally achieved by a numerical procedure. In the course of this paper a linear system of equations is derived by stepwise integration over equidistant intervals. Over a large part of the integration path, Green's functions are regular and are represented by uniformly convergent single series. In the remaining intervals Green's functions are splitted into a regular part and a singular part. The latter is integrated analytically and the result enters the numerical procedure. The regular part is approximated by linear interpolation using the series solution in the basic domain and integrated numerically.

Instead of solving the linear system of equations by a standard procedure, more equations than unknowns may be easily produced and a subsequent least square error procedure renders a smaller system of equations for the unknowns thereby smoothing the distribution of deflections and stresses along the boundary. The size of the system of equations in both cases is generally much smaller than that derived by standard boundary integral equation methods or the Finite

Element Method. One reason for that shall be mentioned: The boundary conditions on part of the boundary are already exactly satisfied by the analytic formulation.

Classical boundary integral equation methods, as described in a recent review article by Christiansen and Hansen [2], make use of Green's function of the infinite domain and therefore the integration path always coincides with the full length of the boundary of the plate. It generally leads to an increase in the number of unknowns which have to be considered in the numerical evaluation of the integral equations. Other problems in the classical formulation namely infinite integration paths arise e.g., in the case of semi-infinite plates, whereas the present method avoids infinite integrations by choosing a proper basic domain.

The procedure is tested in an example problem considering a trapezoidal plate under various boundary conditions. The simply supported case is treated in [3]. As a by-product it is shown that there is no numerical restriction to rigidly clamped plate problems, as was claimed in a somewhat similar formulation in [4]. In a more recent publication [5] an older version of the boundary integral method is used to treat general boundary conditions, see e.g. [6]. The well-known drawback of using line loadings on outer fictitious boundaries in this formulation, however, is the higher computational effort and a loss of accuracy.

Polygonal Plates

A given polygonal plate with arbitrary loading and boundary conditions is embedded in a domain of "simple" planform, thereby applying coincidence of kinematic and dynamic boundary conditions as far as possible. To standardize the method a domain of rectangular shape is chosen for which Green's function w^F is wellknown. The loading of the plate $\overline{p}$ may be extended to the outer domain to form p. Thus, the deflection of the rectangular plate w under that loading can be calculated by means of the Green's function. For some technical important loading functions those deflections are already reported in the literature, see e.g., [7], [12], [14],

$$w(x, y) = \int_{\xi=0}^{a} \int_{\eta=0}^{b} w^F(x, y; \xi, \eta)\, p(\xi, \eta)\, d\xi\, d\eta, \tag{1}$$

where w^F denotes deflection due to a unit force $F = 1$. The basic solutions for the simply supported rectangular plate are listed in Appendix A.

In addition to the above deflections homogeneous solutions w_h have to be superimposed in order to satisfy the boundary conditions along the line of the actual boundary Γ, not already coinciding with the rectangular edges:

$$w_h(x, y) = \int_{\Gamma} w^F(x, y; \sigma)\, \mu^F(\sigma)\, d\sigma + \int_{\Gamma} w^M(x, y; \sigma)\, \mu^M(\sigma)\, d\sigma, \tag{2}$$

where σ denotes arclength of Γ and μ^F, μ^M are unknown lineload densities of external force and moment distributions along Γ, respectively. The second Green's function w^M in Eq. (2) is the deflection of the rectangular plate due to a unit moment loading $M = 1$. The moment vector is oriented parallel to Γ. For definitions and coordinate systems, see Appendix A and Fig. 1.

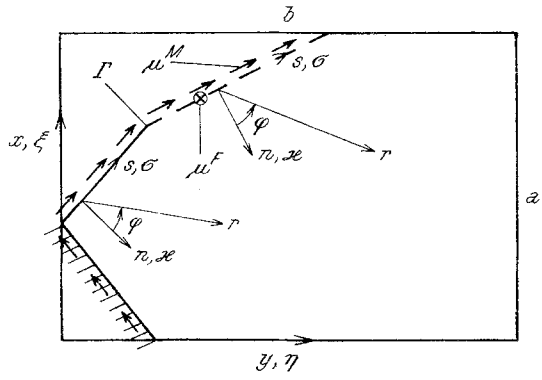

Fig. 1. Geometry of a polygonal plate and a proper basic domain. Definition of density functions along Γ and coordinate systems used in the general formulation. ////////// clamped, ——— simply supported, - - - - free edge

With a proper line load density vector[1], $\boldsymbol{f}^T = (\mu^F, \mu^M)$, the deflection $w + w_h$ in the rectangular domain coincides with the deflection $\overline{w}$ of the polygonal plate, thus satisfying the boundary conditions along Γ at the inner site $n = 0_+$, where n denotes the inner normal coordinate to Γ.

From the boundary conditions prescribed along Γ which form a vector of two components, $\overline{\boldsymbol{Z}}$, a vector integral equation for the line load density vector $\boldsymbol{f}$ is set up:

$$\overline{\boldsymbol{Z}}(s) = \boldsymbol{Z}(s) + \int_{\Gamma} \boldsymbol{G}(s;\sigma)\,\boldsymbol{f}(\sigma)\,d\sigma, \tag{3}$$

where s and σ denote arclength along Γ, and the 2×2 matrix $\boldsymbol{G}$ is Green's matrix corresponding to boundary conditions $\overline{\boldsymbol{Z}}$. The vector $\boldsymbol{Z}$ denotes the corresponding state along Γ in the rectangular plate due to the loading p.

The most important idealized boundary conditions $\overline{\boldsymbol{Z}}$ of classical plate theory are summarized in Table 1. For definitions see Appendix A.

Table 1

Boundary conditions along (some part of) Γ	$\overline{\boldsymbol{Z}}$	$\boldsymbol{G}$
Clamped	$\begin{pmatrix} \overline{w} \\ \overline{w}_{,n} \end{pmatrix} = \boldsymbol{0}$	$\begin{pmatrix} w^F & w^M \\ w^F_{,n} & w^M_{,n} \end{pmatrix}$
Simply supported*	$\begin{pmatrix} \overline{w} \\ \overline{m} \end{pmatrix} = \boldsymbol{0}$	$\begin{pmatrix} w^F & w^M \\ m^F & m^M \end{pmatrix}$
Free	$\begin{pmatrix} \overline{m}_n \\ \bar{q}_n + \overline{m}_{ns,s} \end{pmatrix} = \boldsymbol{0}$	$\begin{pmatrix} m_n{}^F & m_n{}^M \\ q_n{}^F + m^F_{ns,s} & q_n{}^M + m^M_{ns,s} \end{pmatrix}$

* In case of the simply supported straight edge Γ the b.c. $\overline{m}_n = 0$ is conveniently replaced by $\overline{m} = \dfrac{\overline{m}_n + \overline{m}_s}{1+\nu} = \dfrac{\overline{m}_x + \overline{m}_y}{1+\nu} = 0$ and accordingly $m_n{}^F$ and $m_n{}^M$ are replaced by m^F and m^M, respectively.

[1] $\boldsymbol{f}^T$ denotes the transpose of $\boldsymbol{f}$.

The vector integral Eq. (3) may contain singular and non-symmetric kernels, which has to be considered in a numerical solution procedure. In the example problems the following procedure was successful: The boundary Γ is divided into l equidistant intervals of length λ and the unknown line-load density vector becomes stepwise constant in the intervals. By collocation the boundary conditions are thus fullfilled pointwise in the midth of the intervals, s_i $(i = 1, \ldots, l)$. Hence, the integral equations (3) are transformed into a set of $2l$ linear equations for the 2 components of the density vectors $\boldsymbol{f}_j$ $(j = 1, \ldots, l)$:

$$\bar{\boldsymbol{Z}}(s_i) = \boldsymbol{Z}(s_i) + \lambda \sum_{\substack{j=1 \\ j \neq i}}^{l} \boldsymbol{G}(s_i; s_j)\, \boldsymbol{f}_j + \left[\int_{s_i - \lambda/2}^{s_i + \lambda/2} \boldsymbol{G}(s_i, n; \sigma)\, d\sigma \right]_{n=0_+} \boldsymbol{f}_i, \quad (i = 1 \ldots l) \tag{4}$$

where the intervals $j = i$ possibly contain the singularity of $\boldsymbol{G}$. In the non-singular intervals the integrals are replaced by the rectangular-formula, and $\boldsymbol{G}$ is evaluated, e.g., by means of the fast convergent series given in Appendix *A*. To achieve fast convergence also in the case of $|\eta(s_j) - y(s_i)| \to 0$, the second representation of $\boldsymbol{G}$, namely $\hat{\boldsymbol{G}}$ of Appendix A has to be used. The singular integrals in Eq. (4) are calculated by numerical integration of the regular part of $\boldsymbol{G}$, $\boldsymbol{G}_R$, and by analytical integration of the singular part of $\boldsymbol{G}$, $\boldsymbol{G}_S$ where $\boldsymbol{G} = \boldsymbol{G}_S + \boldsymbol{G}_R$. $\boldsymbol{G}_S$ is determined by proper order differentiation of the fundamental solutions of the infinite plate domain,

$$w_\infty^F = \frac{r^2}{8\pi K} \ln \frac{r}{b}, \quad r = [(\sigma - s)^2 + (\varkappa - n)^2]^{1/2}. \tag{5}$$

According to the differential relations and coordinate systems summarized in Appendix *A*, we have e.g.,

$$w_\infty^M = \frac{r}{4\pi K} \ln \frac{r}{b} \cos \varphi, \qquad \varphi = \arctan \frac{\sigma - s}{\varkappa - n}, \tag{6}$$

so that the slope, cf. Table 1, becomes singular,

$$\frac{\partial w_\infty^M}{\partial n} = -\frac{1}{4\pi K} \left[\ln \frac{r}{b} + \cos^2 \varphi \right]. \tag{7}$$

Further differentiation renders the singular Green's functions of the infinite plate, $m_n^{F,M}$, $m^{F,M}$, $q_n^{F,M} + m_{ns,s}^{F,M}$, where the index ∞ is understood. For convenience, the expressions and the results of integration of $\boldsymbol{G}_S$ over the $j = i$-th interval are summarized in Appendix *B*. Being independent of the special choice of the basic domain they are generally applicable.

The regular part $\boldsymbol{G}_R$ is evaluated in the $j = i$-th interval by numerical interpolation of $\boldsymbol{G} - \boldsymbol{G}_S$, using the series solution for $\boldsymbol{G}$ of the rectangular plate in the $j \neq i$-th intervals according to Appendix *A* and the results for $\boldsymbol{G}_S$ presented in Appendix *B*. In the example problem satisfactory results were achieved by linear interpolation and integration of this linear function in the $j = i$-th interval, hence,

$$\int_{s_i - \lambda/2}^{s_i + \lambda/2} \boldsymbol{G}(s_i, n; \sigma)\, d\sigma|_{n=0_+} = \int_{s_i - \lambda/2}^{s_i + \lambda/2} \boldsymbol{G}_S(s_i, n; \sigma)\, d\sigma|_{n=0_+} + \lambda \boldsymbol{G}_R(s_i; s_i). \tag{8}$$

The regular matrix $\boldsymbol{G}_R$ is such a homogeneous solution of the plate equation, as to satisfy the boundary conditions of the rectangular domain for $\boldsymbol{G}$. For a closed form solution using Jacobi's elliptic functions, see [10].

The simple formulation through Eqs. (4) and (8) is numerically satisfactory for not too small λ and as long as the order of singularity in $\boldsymbol{G}_S$ is not too high. In case of the free edge boundary conditions the second order singularity in $(q_n{}^M + m_{ns,s}^M)_\infty$, see Appendix B, unfortunately requires integration of $\boldsymbol{G}_S$ not only in the interval of singularity $j = i$ but also in a few neighboring intervals of the boundary line Γ, also for moderate lengths λ. Saving any change of notation we apply these additional integrations to the whole matrix $\boldsymbol{G}_S$ and find the numerically safe counterpart to Eq. (4):

$$\bar{\boldsymbol{Z}}(s_i) = \boldsymbol{Z}(s_i) + \lambda \sum_{\substack{j=1 \\ j \neq i-\beta}}^{l} \boldsymbol{G}(s_i; s_j)\, \boldsymbol{f}_j + \sum_{j=i-a}^{i+\alpha} \int_{s_j-\lambda/2}^{s_j+\lambda/2} \boldsymbol{G}(s_i, n; \sigma)\, d\sigma|_{n=0_+}\, \boldsymbol{f}_j, \tag{9}$$

$$-\alpha \leqq \beta \leqq \alpha.$$

Test calculations render $\alpha < b/5\lambda$, $b > a$.

Likewise to Eq. (8) we define the integrals in the invervals $i - \alpha \leqq j \leqq i + \alpha$, by

$$\int_{s_j-\lambda/2}^{s_j+\lambda/2} \boldsymbol{G}(s_i, n; \sigma)\, d\sigma|_{n=0_+} = \int_{s_j-\lambda/2}^{s_j+\lambda/2} \boldsymbol{G}_S(s_i, n; \sigma)\, d\sigma|_{n=0_+} + \lambda \boldsymbol{G}_R(s_i; s_j). \tag{10}$$

The integrals of $\boldsymbol{G}_S$ over intervals near $j = i$, namely for $i - \alpha \leqq j \leqq i + \alpha$ for the case of free boundary conditions along a single straight edge are given in Appendix C for convenience. Eqs. (9) and (10) may of course be applied to other boundary conditions at the expense of similar integrations of the proper matrix $\boldsymbol{G}_S$.

A linear system of equations derived from Eq. (4), considering (8) and Appendix B [or equivalently for the free boundary case from Eq. (9) and (10) and in addition Appendix C], is set up for the unknown density vectors $\boldsymbol{f}_i$. After solution of those equations, all kinematical and dynamical components of the state vector in the polygonal plate are calculated by analytical or numerical integration. Considering one of the components which may be denoted by $\bar{e}$ in a point (x, y) within the polygonal plate the integration takes on the form:

$$\bar{e}(x, y) = e(x, y) + \sum_{i=1}^{l} \int_{s_i-\lambda/2}^{s_i+\lambda/2} \boldsymbol{e}^T(x, y; \sigma)\, d\sigma\, \boldsymbol{f}_i, \tag{11}$$

$$\boldsymbol{e}^T = (e^F, e^M).$$

If numerical integration is performed with the rectangular formula, which is appropriate for $e = w, m_x, m_y, m_{xy}$, also for points (x, y) in close distance to the boundary line Γ, it follows

$$\bar{e}(x, y) = e(x, y) + \lambda \sum_{i=1}^{l} \boldsymbol{e}^T(x, y; s_i)\, \boldsymbol{f}_i. \tag{12}$$

Considering the first version of the series solutions of Appendix A for representation of $\boldsymbol{e}$, convergence in the point (x, y) depends on $|\eta(s_i) - y|$. To

establish fast convergence also for $|\eta(s_i) - y| \to 0$, the second representation of $\boldsymbol{e}$, namely $\hat{\boldsymbol{e}}$ of Appendix A has to be used in Eq. (12). Hence, all components $\bar{e}$ in the polygonal plate are directly calculated from their physically corresponding components e and $\boldsymbol{e}$ in the basic (rectangular) domain. No numerical differentiation is needed.

Application of Eq. (12) may become numerically unsafe near the boundary line Γ. The distance of points (x, y) to Γ must be kept larger if the vector $\boldsymbol{e}^T(x, y; s_i)$ becomes singular at the boundary. For the higher order singularity of the shearing force discussed above Eq. (11) should be integrated analogously to Eq. (10) to get the points (x, y) closer, if required, to the boundary line Γ.

Example Problems

To test the method, plates of trapezoidal planform with rectangular corners are considered, see Fig. 2a where for some special geometries and uniform pressure loading analytically derived solutions have been published, e.g. in [7], [11] and [12] which are compared to the numerical solution. Therefore, the following boundary conditions are applied:

1. Navier boundary conditions at 4 edges. In [11] analytically derived results may be found for a skewness angle $\gamma = \pi/3$ and $a/b = \sqrt{3}/2$ and in [12, p. 179], results are given for a triangular plate where $\gamma = \pi/4$ and $a/b = 1$.

2. Navier boundary conditions at 3 edges, the skew edge is free. In [14, p. 211] and [15, p. 406], a rectangular plate is considered.

According to those boundary conditions the "best" basic domain is a rectangular plate with simply supported edges, see Fig. 1. The unknown line load densities μ^F and μ^M are applied at the skew edge line Γ. Considering Eq. (4) and (8) along Γ, a linear system of equations for the discretized density functions is derived. According to the coordinate systems of Fig. 2a, evaluations are made at equidistant points of Γ,

$$s_i = (2i - 1)\,\lambda/2, \qquad i = 1, \ldots, l.$$

The Green's function of the rectangular plate is given in Appendix A and enters the numerical procedure where the infinite series solutions in the intervals $j \neq i$ are approximated by finite sums. To keep the error small test calculations have to be performed.

The following hints may be helpful. For numerical convenience the hyperbolic functions entering the series solutions are resolved into their exponential function representations and exponentials with positive argument are eliminated. It is seen that the speed of convergence of the series given in the first version of Appendix A is determined by $\exp -\alpha_n\,|\eta(s_j) - y(s_i)|$ and in the second version by $\exp -\beta_n\,|\xi(s_j) - x(s_i)|$, respectively. The first finite version is prefered for $b > a$ and may be used with a reasonable number of about 100 terms up to skewness angles of $\gamma = \pi/3$. Then the maximal error in the most severe case of the shearing force $q_n{}^M$, when evaluated in intervals neighboring the singularity, is kept less than $1^0/_{00}$, where $\lambda/b = 1/19$ and $a/b = \sqrt{3}/2$. Although the restriction to 100 terms is superficial with respect to computing, switching to the second

version of the series is recommended for $\gamma > \pi/3$. In such a computer program those switches can be performed by proper changes in coordinates and parameters of the first version of the series representing the deflections $w^{F,M}$ and their derivatives with respect to x and y. Therefore, it is not necessary to program the analytical second version of the series.

The integrals of the singular parts of the Green's functions over the $j = i$-th inverval in Eq. (8) which are independent of the basic domain are taken from Appendix *B*. The regular part of the Green's functions in the interval $j = i$ is approximated by numerical (linear) interpolation using the values of $\boldsymbol{G} - \boldsymbol{G}_S$ in the neighboring intervals $j = i - 1$, $j = i + 1$, where $\boldsymbol{G}$ is evaluated approximately by summing the finite series as discussed before, for intervals $j \neq i$.

Thus, the system matrix of Eq. (4) is determined and naturally consists of four $l \times l$ submatrices according to Table 1, where the coefficients in the main diagonals are dominating due to the contributions of the singular integrals.

The vector of inhomogeneity $\boldsymbol{Z}$ is evaluated in the points s_i of Γ in the rectangular domain and may be taken from the literature, e.g. [7], [12], [14], or is calculated from Eq. (1) by means of the Green's functions. The vector $\overline{\boldsymbol{Z}} = \boldsymbol{0}$ in case of the above mentioned boundary conditions.

A proper choice of l renders the size $2l$ of the system of equations. The linear equations are well behaved and are solved by standard procedures. If necessary a reduction in the number of unknowns may be achieved by considering the line load density vector constant over several intervals. Thus, the coefficients matrix becomes rectangular and Eq. (4) is then multiplied from the left by the transposed of the coefficients matrix. The resulting system is of smaller size than $2l$ and renders a solution which is smoothed along Γ in the least-square sense, cf. [13].

Having evaluated the line load density vectors $\boldsymbol{f}_i$, deflections and moments are calculated in the trapezoidal plate from Eq. (10) using the corresponding solutions and Green's functions in the rectangular domain, e.g. for $\bar{e} \equiv \overline{m}_x$:

$$\overline{m}_x = m_x + \lambda \sum_{i=1}^{l} (m_x{}^F, m_x{}^M) \cdot \boldsymbol{f}_i. \tag{13}$$

At a point (x, y) evaluation of $(m_x{}^F, m_x{}^M)$ is performed according to the finite series derived from Appendix *A*. For points s_i of Γ, where $|\eta(s_i) - y|$ is not too small the first version of Green's functions is fast convergent. For points s_i of Γ, where $|\eta(s_i) - y| \to 0$, however, switching to the second version of the series $(\hat{m}_x{}^F, \hat{m}_x{}^M)$ has to be made, analogous to the procedure described above for the generation of the system matrix. If there is only one such point s_i of Γ, switching may be avoided and replaced by numerical interpolation of the Green's functions computed in the first version in the neighboring intervals $(i - 1, i + 1)$.

Only in the close vicinity of the skew boundary line Γ the numerical results of Eq. (11) become unreliable due to the poor convergence of both versions of the series $(m_x{}^F, m_x{}^M)$ and the approximation of the boundary conditions along Γ; at the other coinciding edges the boundary conditions are identically satisfied.

From the test calculations it is concluded that the method renders satisactory numerical results already for a rather large length λ of the intervals. In Table 2 the results and errors are given for $l = 19$ intervals. In Figs. 2 to 5 the influence of the skew angle γ is studied.

Table 2

	ad. 1: Navier boundary conditions					
	Trapezoidal plate $\gamma = \pi/3,\ a/b = \sqrt{3}/2$ $x = 0{,}4076\,b$ $y = 0{,}5897\,b$			Triangular plate $\gamma = \pi/4,\ a/b = 1$ $x = 0{,}3158\,b$ $y = 0{,}6824\,b$		
	$l = 19$	Mang [11]	error %	$l = 19$	Nadai [12, p. 179]	error %
$\frac{K}{\bar{p}b^4}\,\bar{w} \cdot 10^4$	14,6	14,6	0	6,45	6,56	−1,67
$\frac{1}{\bar{p}b^2}\,\bar{m} \cdot 10^2$	4,380	4,410	−0,68	2,901	2,946	−1,53

	ad. 2: Three edges simply supported, one edge free			
	Rectangular plate $a/b = 1,\ \bar{a}/b = \frac{1}{2},\ \bar{b} = b;$ $\nu = 0{,}3$			
	$l = 19$	Timoshenko [14, p. 212]	error %	
$\frac{K}{\bar{p}b^4}\,\bar{w} \cdot 10^4$	72,0	71,0	1,41	$x = \bar{a}$ $y = 0{,}5\,\bar{b}$
$\frac{1}{\bar{p}b^2}\,\bar{m} \cdot 10^2$	4,692	4,692	0	$x = 0{,}5\,\bar{a}$ $y = 0{,}5\,\bar{b}$
	Rectangular plate, $a/b = 1,\ \bar{a}/b = \frac{1}{2},\ \bar{b} = b;$ $\nu = 0$			
	$l = 19$	Czerny [15, p. 406]	error %	
$\frac{K}{\bar{p}b^4}\,\bar{w} \cdot 10^4$	55,8	55,2	1,08	$x = \bar{a}$ $x = 0{,}5\,\bar{b}$
$\frac{1}{\bar{p}b^2}\,\bar{m}_x \cdot 10^2$	1,916	1,924	−0,41	$x = 0{,}5\,\bar{a}$ $y = 0{,}5\,\bar{b}$
$\frac{1}{\bar{p}b}\,(\bar{q}_x + \bar{m}_{xy,y})$	0,4357	0,4348	0,21	$x = 0$ $y = 0{,}5\,\bar{b}$

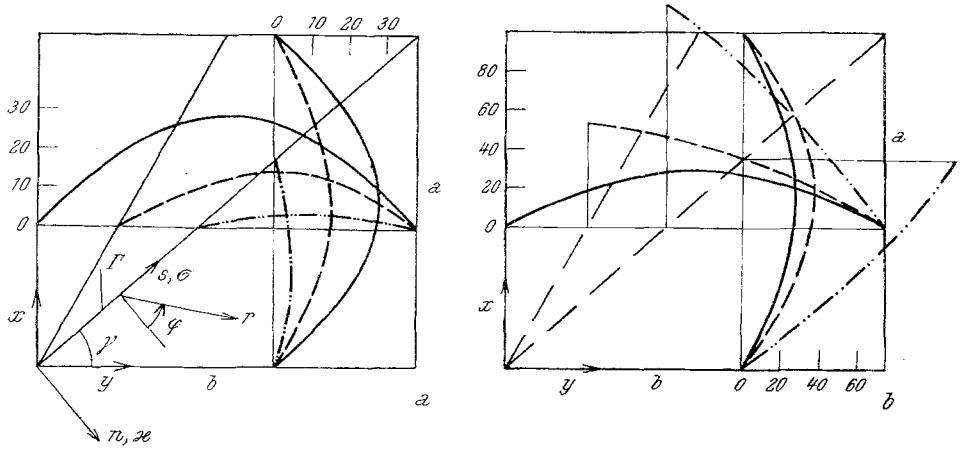

Fig. 2. Dimensionless deflection, $\frac{K}{\bar{p}b^4}\,\bar{w}\cdot 10^4$, under uniform pressure loading $\bar{p}$. $\frac{x}{a}=\frac{5}{12}$ and $\frac{y}{b}=\frac{5}{8}$, respectively. $a/b=\sqrt{3}/2$. ——— rectangular plate, - - - - trapezoidal plate, ····· triangular plate. *a* Navier boundary conditions on all 4 edges. Definition of coordinates in case of the triangular plate, *b* Skew edge free, the other edges simply supported. $\nu=0{,}3$

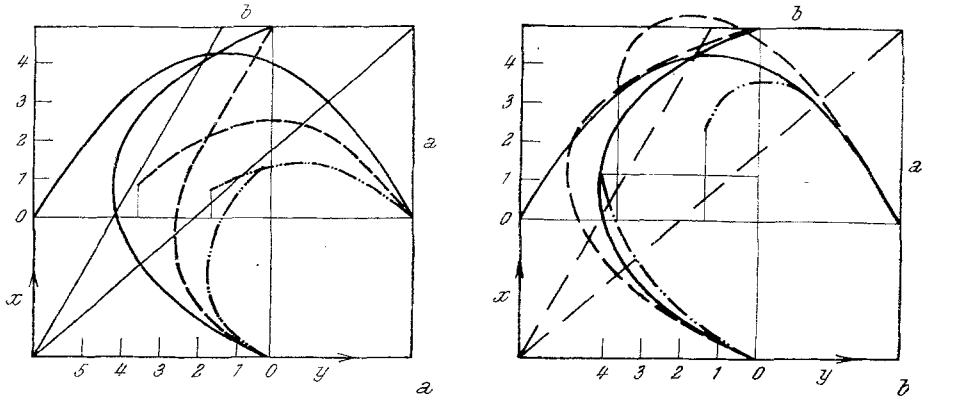

Fig. 3. Dimensionless moment, $\frac{1}{\bar{p}b^2}\,\bar{m}_x\cdot 10^2$, under uniform pressure loading $\bar{p}$. $\frac{x}{b}=\frac{5}{12}$ and $\frac{y}{b}=\frac{5}{8}$, respectively. $a/b=\sqrt{3}/2$. ——— rectangular plate, - - - - trapezoidal plate, ····· triangular plate. *a* Navier boundary conditions on all 4 edges. $\nu=0{,}3$, *b* Skew edge free, the other edges simply supported. $\nu=0{,}3$

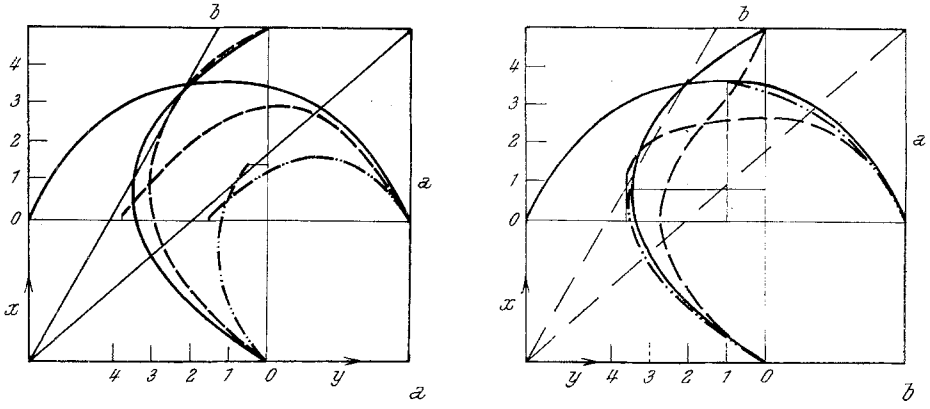

Fig. 4. Dimensionless moment, $\frac{1}{\bar{p}b^2}\,\bar{m}_y \cdot 10^2$, under uniform pressure loading $\bar{p}$. $\frac{x}{b} = \frac{5}{12}$ and $\frac{y}{b} = \frac{5}{8}$, respectively. $a/b = \sqrt{3}/2$. ——— rectangular plate, - - - - trapezoidal plate, ····· triangular plate. *a* Navier boundary conditions on all 4 edges. $\nu = 0{,}3$, *b* Skew edge free, the other edges simply supported. $\nu = 0{,}3$

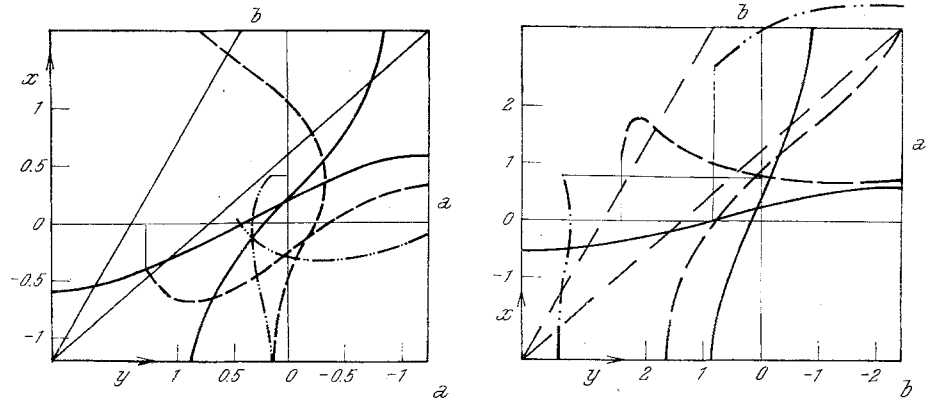

Fig. 5. Dimensionless moment, $\frac{1}{\bar{p}b^2}\,\bar{m}_{xy} \cdot 10^2$, under uniform pressure leading $\bar{p}$. $\frac{x}{b} = \frac{5}{12}$ and $\frac{y}{b} = \frac{5}{8}$, respectively. $a/b = \sqrt{3}/2$. ——— rectangular plate, - - - - trapezoidal plate, ····· triangular plate. *a* Navier boundary conditions on all 4 edges. $\nu = 0{,}3$, *b* Skew edge free, the other edges simply supported. $\nu = 0{,}3$

A FORTRAN-program was set-up and implemented in the CYBER 74 computer of the Technical University of Vienna. Evaluation of deflections and moments in 10 points took approximately 35 seconds CPA which seems to be very cost effective.

Concluding Remarks

The main result is represented by the vector integral Eq. (3) which is derived by the Green's function method using a basic domain. Integration runs over that part Γ of the actual boundary where boundary conditions are not already satisfied. Applying the rectangular formula renders Eqs. (4) or (9). Thus, using the ideas of Eqs. (8) or (10), an economic numerical procedure is formulated. Integrals over singular intervals are evaluated independently of the basic domain and are listed in Appendix *B* and *C*. The corresponding system of linear equations is generally well behaved and may be solved by standard procedures. A simple computer program can be designed and computing costs are comparatively inexpensive. Deflections and moments are evaluated pointwise by Eq. (10) directly using the proper functions of the basic domain. Hence, no numerical differentiation is necessary.

The advantage of the problem oriented numerical method is also manifest in the fact that with respect to the basic domain only boundary perturbations are considered. However, the common diasdvantage generally observed in numerical methods is also inherent in this paper — moments cannot be evaluated in a close vicinity of the non-coinciding boundary Γ.

Appendix A

Green's functions of a rectangular plate $[a, b]$ with Navier boundary conditions can be taken from the literature. Hence, the deflection in (x, y) due to a unit force $F = 1$ applied at the point (ξ, η) is, for $\eta \geqq y$, given by

$$w^F = \frac{a^2}{K\pi^3} \sum_{n=1}^{\infty} (1 + \alpha_n b \coth \alpha_n b - \alpha_n \eta' \coth \alpha_n \eta' - \alpha_n y \coth \alpha_n y) \cdot \sinh \alpha_n \eta' \sinh \alpha_n y \sin \alpha_n \xi \sin \alpha_n x / n^3 \sinh \alpha_n b,$$

$$\eta' = b - \eta, \qquad y' = b - y, \qquad \alpha_n = n\pi/a.$$

For $\eta \leqq y$ replace (η', y) by (η, y').

The deflection in (x, y) due to a unit moment $M = 1$ applied at the point (ξ, η), with the moment vector pointing in the direction of Γ, which enters the formulation in Eq. (2), may be calculated from w^F by differentiation, according to Nemenyi [8]:

$$w^M(x, y; \xi, \eta) = w^F_{,\varkappa}(\xi, \eta; x, y), \quad \text{where} \quad \xi = \xi(\sigma, \varkappa), \quad \eta = \eta(\sigma, \varkappa).$$

Here, σ and $\varkappa$ denote coordinates of the point of application of M, measured along Γ and along the inner normal of Γ, respectively. A coinciding coordinate-system to $(\sigma, \varkappa)$ is denoted by (s, n), see Fig. 1.

Moments and the shearing force are defined by differentiation with respect to the field point coordinates (s, n). For the isothermal case we have:

$$m_n = -K(w_{,nn} + \nu w_{,ss}),$$
$$m_s = -K(w_{,ss} + \nu w_{,nn}),$$
$$m_{ns} = -K(1-\nu)\, w_{,ns},$$
$$q_n = -K\Delta w_{,n},$$

where $K = Eh^3/12(1-\nu^2)$ denotes bending stiffness.

Those series representations of the Green's function become poorly convergent for $|\eta - y| \to 0$, especially for the higher order derivatives of the deflections $w^{F,M}$. Generally, in the literature the above formulation is used for $b \geqq a$ for the sake of fast convergence for $\eta \neq y$. Since the original Navier double sum representation is symmetric another single series may be derived in an analogous manner, for $\xi \geqq x$,

$$\hat{w}^F = \frac{b^2}{K\pi^3} \sum_{n=1}^{\infty} (1 + \beta_n a \coth \beta_n a - \beta_n \xi' \coth \beta_n \xi' - \beta_n x \coth \beta_n x)$$
$$\cdot \sinh \beta_n \xi' \sinh \beta_n x \sin \beta_n \eta \sin \beta_n y / n^3 \sinh \beta_n a,$$
$$\xi' = a - \xi, \qquad x' = a - x, \qquad \beta_n = n\pi/b.$$

For $\xi \leqq x$ replace (ξ', x) by (ξ, x'). Although, convergence becomes now poor for $b \gg a$, the series is sufficiently well suited for the case $|\eta - y| \to 0$, $|\xi - x|$ not too small and for b/a not too large.

Appendix B

Table of singular components of $\boldsymbol{G}$ and their integrals over the $j = i$-th interval of length λ on Γ, calculated from Eq. (5) and the formulas of Appendix A; $r = [(\sigma - s)^2 + (\varkappa - n)^2]^{1/2}$, $\varphi = \arctan \dfrac{\sigma - s}{\varkappa - n}$. The limes $n = 0_+$ is performed after integrating $\boldsymbol{G}_S$, see Fig. 1.

Appendix C

Table of the integrals of singular components of $\boldsymbol{G}$ for the case of free boundary conditions over the $j = (i - \beta)$-th interval of length λ on Γ, calculated from the formulas of Appendix B.

$$4\pi\lambda \int_{\left(s_j - \frac{\lambda}{2}\right)}^{\left(s_j + \frac{\lambda}{2}\right)} \boldsymbol{G}_S(s_i, n; \sigma)\, d\sigma|_{n=0_+}$$

$$\begin{pmatrix} -(1+\nu)\,\lambda^2 \left[\ln \frac{\lambda}{2b}\sqrt{q_1|q_2|} - (1-\nu)/2(1+\nu) + |\beta| \ln q_1/|q_2|\right] & 2\pi\lambda q_3 \\ -2\pi\lambda q_3 & -4(1+\nu)/q_1 q_2 \end{pmatrix},$$

where $q_1 = 1 + 2\,|\beta|$, $q_2 = 1 - 2|\beta|$, $q_3 = \begin{cases} 0, \ldots, \beta \neq 0 \\ 1, \ldots, \beta = 0 \end{cases}$.

Boundary condition in the $j = i$-th interval of Γ	$8\pi \boldsymbol{G}_S$
Clamped	$\begin{pmatrix} 0 & 0 \\ 0 & \frac{-2}{K}\left(\ln\frac{r}{b} + \cos^2\varphi\right) \end{pmatrix}$
Simply supported	$\begin{pmatrix} 0 & 0 \\ -4\left(\ln\frac{r}{b} + 1\right) & -4\frac{\cos\varphi}{r} \end{pmatrix}$
Free	$\begin{pmatrix} -\left[(1+\nu)\left(2\ln\frac{r}{b} + 1\right) + 2(\cos^2\varphi + \nu\sin^2\varphi)\right] & -2\frac{\cos\varphi}{r}\left[2 - (1-\nu)\cos 2\varphi\right] \\ 2\frac{\cos\varphi}{r}\left[2 + (1-\nu)\cos 2\varphi\right] & -\frac{2}{r^2}\left[2\cos 2\varphi + (1-\nu)\cos 4\varphi\right] \end{pmatrix}$
	$4\pi\lambda \int_{(s_i-\lambda/2)}^{(s_i+\lambda/2)} \boldsymbol{G}_S(s_i, n; \sigma)\, d\sigma\vert_{n=0_+}$
Clamped	$\begin{pmatrix} 0 & 0 \\ 0 & -\frac{\lambda^2}{K}\left(\ln\frac{\lambda}{2b} - 1\right) \end{pmatrix}$
Simply supported	$\begin{pmatrix} 0 & 0 \\ -2\lambda^2\ln\frac{\lambda}{2b} & 2\pi\lambda \end{pmatrix}$
Free	$\begin{pmatrix} -(1+\nu)\lambda^2\left[\ln\frac{\lambda}{2b} - (1-\nu)/2(1+\nu)\right] & 2\pi\lambda \\ -2\pi\lambda & -4(1+\nu) \end{pmatrix}$

References

[1] Melnikov, Yu. A.: Some applications of the Green's function method in mechanics. Int. J. Solids Structures **13**, 1045–1058 (1977).

[2] Christiansen, S., Hansen, E. B.: Numerical solution of boundary value problems through integral equations. ZAMM **58**, T14–T25 (1978).

[3] Irschik, H.: Ein Integralgleichungsverfahren zur Berechnung allseits frei drehbar gelagerter Trapezplatten mit rechten Winkeln. ZAMM **60**, T125–T127 (1980).

[4] Altiero, N. J., Sikarskie, D. L.: A boundary integral method applied to plates of arbitrary plan form. Computers & Structures **9**, 163–168 (1978).

[5] Wu, B. C., Altiero, N. J.: A boundary integral method applied to plates of arbitrary plan form and arbitrary boundary conditions. Computers & Structures **10**, 703–707 (1979).

[6] Chicurel, R., Suppiger, E. W.: The reflection method in elasticity and bending of plates. ZAMP **15**, 629–638 (1964).

[7] Bittner, E.: Platten und Behälter. Wien—New York: Springer 1965.
[8] Nemenyi, P.: Eine neue Singuläritätenmethode für die Elastizitätstheorie. ZAMM **9**, 488—490 (1929).
[9] Altenbach, J.: Die Berechnung ebener Flächentragwerke mit Hilfe von Einflußfunktionen zugeordneter vereinfachter Grundaufgaben. ZAMM **52**, T288—T292 (1972).
[10] Toelke, F.: Über Spannungszustände in dünnen Rechteckplatten. Ing.-Archiv **5**, 187—237 (1934).
[11] Mang, H.: Trapezplatten mit rechten Winkeln. — Ein Beitrag zur funktionentheoretischen Berechnung von Plattentragwerken. Der Stahlbau **43**, 141—146, 242—248 (1974).
[12] Nadai, A.: Die elastischen Platten. Berlin: Springer 1925.
[13] Noble, B.: Applied linear algebra. Englewood Cliffs, N.J.: Prentice-Hall 1969.
[14] Timoshenko, S., Woinowsky-Krieger, S.: Theory of plates and shells, 2nd ed. New York: McGraw-Hill 1959.
[15] Czerny, F.: Tafeln für vierseitig und dreiseitig gelagerte Rechteckplatten, in: Beton-Kalender. Berlin: W. Ernst & Sohn 1978.

Univ.-Ass. Dipl.-Ing. H. Irschik and Prof. Dipl.-Ing. Dr. F. Ziegler
Institut für Allgemeine Mechanik
Technische Universität Wien
Karlsplatz 13
A-1040 Wien, Austria